



Greenwich Academic Literature Archive (GALA)
– the University of Greenwich open access repository
<http://gala.gre.ac.uk>

Citation for published version:

Lu, Yun-Long, Dai, Gao-Le, Wang, Yi, Liu, Taijun and Huang, Jifu (2016) Dual-Band Filtering Power Divider With Capacitor-Loaded Centrally Coupled-Line Resonators. IET Microwaves, Antennas & Propagation. ISSN 1751-8725 (In Press) (doi:10.1049/iet-map.2016.0217)

Publisher's version available at:

Please note that where the full text version provided on GALA is not the final published version, the version made available will be the most up-to-date full-text (post-print) version as provided by the author(s). Where possible, or if citing, it is recommended that the publisher's (definitive) version be consulted to ensure any subsequent changes to the text are noted.

Citation for this version held on GALA:

Lu, Yun-Long, Dai, Gao-Le, Wang, Yi, Liu, Taijun and Huang, Jifu (2016) Dual-Band Filtering Power Divider With Capacitor-Loaded Centrally Coupled-Line Resonators. London: Greenwich Academic Literature Archive.
Available at: <http://gala.gre.ac.uk/15617/>

Contact: gala@gre.ac.uk

Dual-Band Filtering Power Divider With Capacitor-Loaded Centrally Coupled-Line Resonators

Yunlong Lu^{1*}, Gaole Dai², Yi Wang³, Taijun Liu¹ and Jifu Huang¹

¹ Faculty of Electrical Engineering and Computer Science, Ningbo University, Ningbo, Zhejiang, 315211, China

² Ningbo Institute of Materials Technology & Engineering, Chinese Academy of Sciences, Ningbo 315201, China

³ Department of Engineering Science, University of Greenwich, ME4 4TB, Kent, UK

* luyunlong@nbu.edu.cn

Abstract: In this paper, a dual-band filtering power divider (DB-FPD) with capacitor-loaded centrally coupled-line resonators (CLCCLRs) is presented. The proposed design utilizes four CLCCLRs, two resistors and one inductor to achieve the dual functions of dual-band filtering and power division. By altering the values of the capacitors loaded at the ends of the coupled-lines, the center frequencies of the two passbands can be adjusted independently. It is noted that changing one passband will not affect the other. For demonstration, a microstrip filtering power divider is designed, fabricated and measured. Under different values of the loaded capacitors, experimental results show that the lower band center frequency varies from 0.7 GHz to 1.0 GHz with the upper band fixed at 1.75 GHz, whereas the upper band center frequency varies from 1.65 GHz to 1.95 GHz when the lower band is fixed at 1.0 GHz. The measured results show good agreement with the simulations.

1. Introduction

With the rapid development of modern wireless communication services, wireless devices with dual-/multi-band and multiple functions within a limited circuit area are increasingly in high demand [1]. Integrating various RF functions at different operating frequencies into one component becomes an attractive design concept for circuit miniaturization. For instance, a power divider (PD) and a bandpass filter (BPF), as the essential blocks in many wireless communication systems, can be merged when they coexist in the front-end to realize compact size and high performances. A lot of efforts to integrate PDs and BPFs have been made recently [2]-[20]. A straightforward way is to cascade the filtering structure with a Wilkinson PD [2]-[4]. However, with this approach, the circuits still occupy a fairly large space. An alternative method is to use coupling sections or filtering structures to replace the quarter-wavelength impedance transformers in conventional PDs [5]-[14]. The above mentioned works focused on single band operations. For concurrent dual-band wireless systems, dual-band filtering power dividers (DB-FPDs) are desired [15]-[19]. In [15] a dual-band filtering structure was proposed using centrally loaded resonators, whereas in [16] transversal filtering sections were embedded in Wilkinson PDs to obtain the functions of

This article has been accepted for publication in a future issue of this journal, but has not been fully edited.

Content may change prior to final publication in an issue of the journal. To cite the paper please use the doi provided on the Digital Library page.

single/multi-band filtering and power division. In [17]-[19], stepped impedance resonators and stub-loaded resonators are utilized to substitute quarter-wavelength transmission lines to achieve the DB-FPDs.

In this paper, we propose a novel structure of DB-FPD with independently controllable center frequencies. In the proposed topology, four capacitor-loaded centrally coupled-line resonators (CLCCLRs) and three lumped elements are arranged to form a filtering power-division network. Even-/odd-mode method is applied to analyze the filtering and power divider responses. Theoretical analysis shows that the center frequencies of the dual passbands can be independently controlled by altering the values of corresponding loaded capacitors. This is then verified by both simulations and experiments.

2. Analysis and design

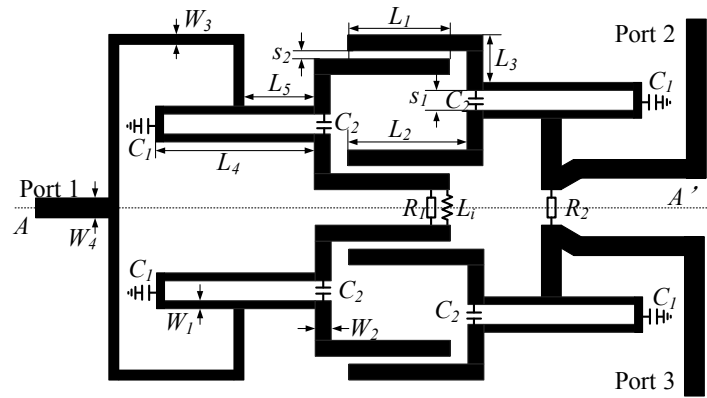


Fig. 1. Configuration of the proposed DB-FPD

Fig. 1 shows the proposed DB-FPD. Four CLCCLRs are arranged symmetrically to replace the two quarter-wavelength transmission lines of a conventional power divider. Each CLCCLR consists of a centrally coupled-line resonator and two capacitors C_1 and C_2 . Two resistors (R_1 and R_2) and an inductor (L_i) work as the isolation elements and do not affect the filtering responses [15]. Since the structure of the proposed circuit is symmetrical with respect to the $A-A'$ plane, the even- and odd-mode analysis is applied. The three-port scattering parameters can be theoretically obtained as follows [20]:

$$S_{11} = S_{11}^e \quad (1a)$$

$$S_{21} = S_{31} = \frac{S_{12}^e}{\sqrt{2}} \quad (1b)$$

$$S_{23} = \frac{(S_{22}^e - S_{22}^o)}{2} \quad (1c)$$

$$S_{22} = S_{33} = \frac{(S_{22}^e + S_{22}^o)}{2} \quad (1d)$$

This article has been accepted for publication in a future issue of this journal, but has not been fully edited.

Content may change prior to final publication in an issue of the journal. To cite the paper please use the doi provided on the Digital Library page.

where S_{ij}^e and S_{ij}^o are the scattering parameters of the even- and odd-mode equivalent circuits. It should be noted that the trans-mission coefficients (S_{21} and S_{31}) and reflection coefficient S_{11} are only related to the even-mode equivalent circuit.

2.1. Properties of the CLCCLR resonator

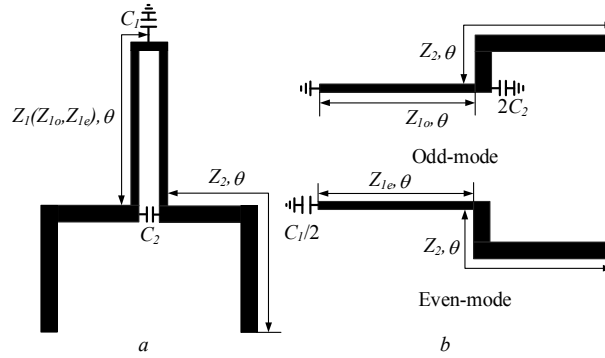


Fig. 2. Proposed resonator

a Structure of the CLCCLR

b Odd- and even-mode equivalent circuits of the CLCCLR

The structure of the CLCCLR is shown in Fig. 2(a), a capacitor C_1 is loaded at the center of the resonator, whereas another capacitor C_2 is added across the ends of the coupled-line. Due to its symmetry, the resonator can also be analyzed using the odd- and even-mode analysis as shown in Fig. 2(b), where Z_1 and Z_2 denote the characteristic impedances and θ represents the electrical length of the microstrip line. The input admittances of odd- and even-mode equivalent circuits can be expressed as:

$$Y_{odd} = \frac{j \tan \theta}{Z_2} + \frac{1}{jZ_{1o} \tan \theta} + j\omega(2C_2) \quad (2)$$

$$Y_{even} = \frac{j \tan \theta}{Z_2} + \frac{\omega C_1 Z_{1e} + 2 \tan \theta}{j(-2Z_{1e} + \omega C_1 Z_{1e}^2 \tan \theta)} \quad (3)$$

Applying the resonance condition $Y_{odd/even} = 0$, the odd- and even-mode resonant frequencies of the proposed resonator can be obtained as:

$$-\frac{\tan \theta}{Z_2} + \frac{1}{Z_{1o} \tan \theta} - \omega(2C_2) = 0 \quad (4)$$

$$\frac{\tan \theta}{Z_2} - \frac{\omega C_1 Z_{1e} + 2 \tan \theta}{(-2Z_{1e} + \omega C_1 Z_{1e}^2 \tan \theta)} = 0 \quad (5)$$

where Z_{1o} and Z_{1e} represent the odd- and even-mode characteristic impedances of the coupled line in the CLCCLR resonator. Once the physical dimensions are fixed, the even- and odd-mode resonant frequencies of the CLCCLR can be independently adjusted by C_1 and C_2 . As shown in Fig. 3, with C_1 being fixed f_{odd} is shifted down as C_2 increases, whereas f_{even} is shifted down as C_1 increases with C_2 being fixed. As a

This article has been accepted for publication in a future issue of this journal, but has not been fully edited.

Content may change prior to final publication in an issue of the journal. To cite the paper please use the doi provided on the Digital Library page.

result, the f_{even} and f_{odd} can be adjusted independently by altering C_1 and C_2 , respectively. Next, the DB-FPD will be analyzed using the even- and odd-model method.

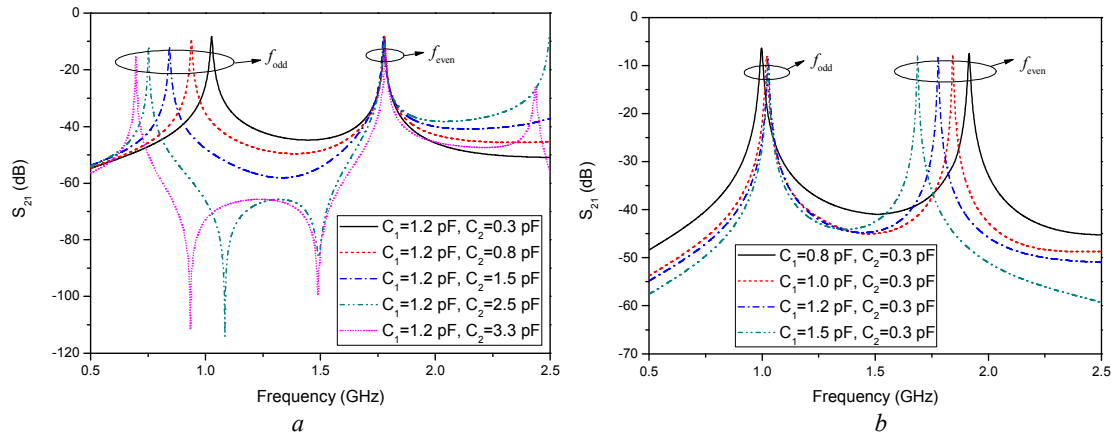


Fig. 3. Independent change of the even- and odd-mode resonant frequencies of the CLCCLR resonator as C_1 and C_2 vary, respectively

a C_2 varies while C_1 fixed at 1.2 pF

b C_1 varies while C_2 fixed at 0.3 pF

2.2. Even-mode analysis of the DB-FPD

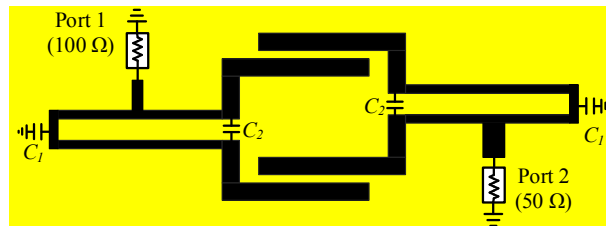


Fig. 4. Even-mode equivalent circuit of the DB-FPD

When the even-mode is excited at ports 2 and 3, the equivalent circuit can be reduced to Fig. 4. From equations (1a)-(1d), the even-mode equivalent circuit determines the transmission responses and input matching at port 1 of the DB-FPD. In this case, the input impedance at port 1 is 100 Ω . The equivalent circuit in Fig. 4 is designed and optimized to produce a 2nd-order filter response. At the center operating frequencies of the even-mode equivalent filtering circuit, the phase shifts are 90°, which demonstrates the filter’s property. Due to the filter’s phase-shift characteristic, it can be matched to any impedance to meet different demands and provides a good impedance matching at port 1 [15]. Besides, for the filter design, the coupling coefficients and external quality factors should be considered. The coupling coefficients can be calculated as [20]:

$$k = \frac{f_2^2 - f_1^2}{f_2^2 + f_1^2} \quad (6)$$

This article has been accepted for publication in a future issue of this journal, but has not been fully edited.

Content may change prior to final publication in an issue of the journal. To cite the paper please use the doi provided on the Digital Library page.

where f_1 and f_2 are the two resonant frequencies of the coupled resonators. The external quality factor (Q_e) is determined by the tap position of the feeding structure, which can be obtained by [20]:

$$Q_e = \frac{f_0}{\Delta f_{\pm 90^\circ}} \quad (7)$$

where f_0 denotes the fundamental resonant frequency, $\Delta f_{\pm 90^\circ}$ is the bandwidth of the resonant frequency over which the phase shifts $\pm 90^\circ$. Since the impedance of port 1 becomes 100Ω under the even-mode excitation, when extracting the coupling coefficients and external quality factors, the impedance of port 1 should be set as 100Ω in simulation [8]. The extracting methods of coupling coefficients and external quality factors based on CLCCLRs in a 50Ω system have been detailed in our previous work [21].

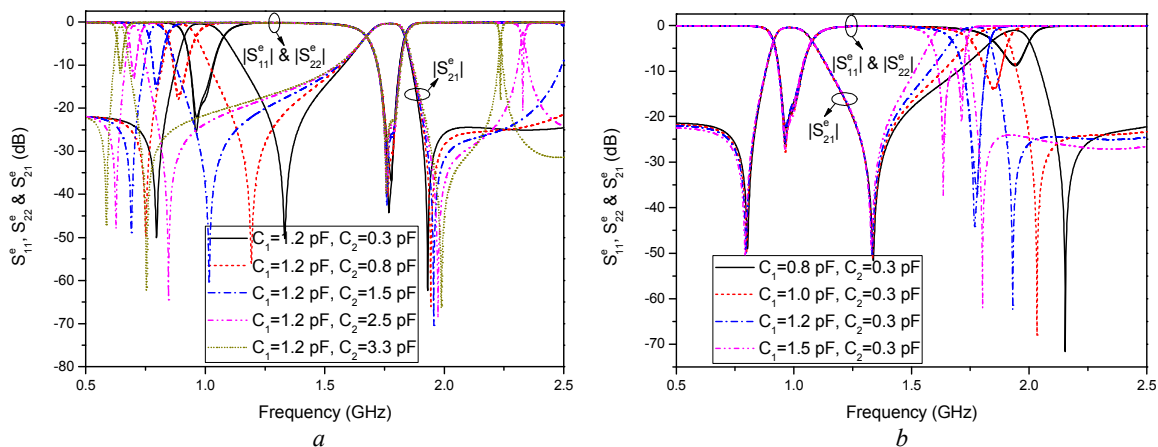


Fig. 5. Simulated filtering responses of the even-mode circuit under different loaded-capacitors

a fixed C_1 and variable C_2 from 0.3 to 3.3 pF

b fixed C_2 and variable C_1 from 0.8 to 1.5 pF

Fig. 5 shows the even-mode responses as a function of the loaded capacitors C_1 and C_2 . It can be seen that the center frequencies of the dual passbands can be independently controlled by C_1 and C_2 . In addition, three transmission zeros located at the lower and upper skirts of the dual passbands are obtained to enhance the selectivity. The first two transmission zeros are created by the two unequal arms from the tapping point to the ends of the CLCCLR that roughly correspond to quarter of a guided wavelength at the frequencies of the two zeros. The last one is created by the path between the tapping position and the grounded end of the capacitor C_1 , as the input impedance viewed from the tapping position to the capacitor approaches zero at the frequency of this transmission zero [22]. Once the even-mode circuit is achieved, the independently controllable dual-band filtering responses of the power divider are guaranteed. Next, to achieve the matching and isolation at the output ports, the odd-mode circuit will be analyzed.

2.3. Odd-mode analysis of the DB-FPD

This article has been accepted for publication in a future issue of this journal, but has not been fully edited.

Content may change prior to final publication in an issue of the journal. To cite the paper please use the doi provided on the Digital Library page.

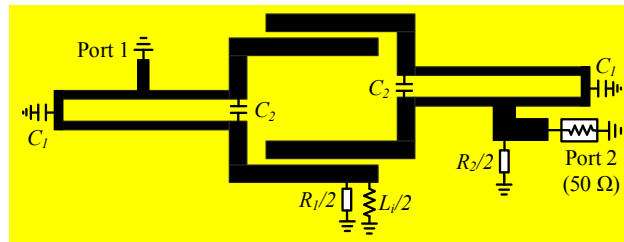


Fig. 6. Odd-mode equivalent circuit of the DB-FPD

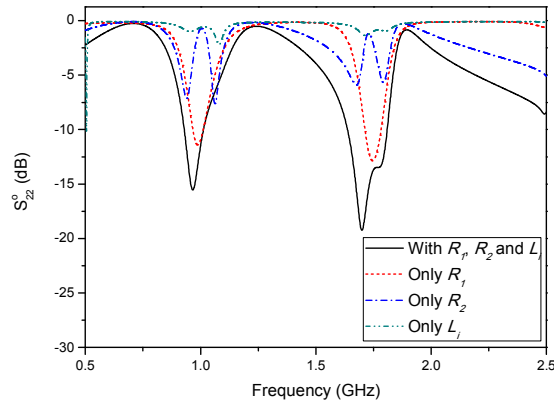


Fig. 7. Simulated S -parameters of the odd-mode circuit with different isolation elements combination under $C_1=1.2$ pF and $C_2=0.3$ pF

When the odd-mode excitation is applied to ports 2 and 3, port 1 is short-circuited due to the node voltage being equal to zero. The equivalent circuit can be deduced as shown in Fig. 6. From the view of the power divider, the odd-mode equivalent circuit functions as an impedance transformer that converts the shunt isolation elements to match the port 2 and therefore achieves a good isolation. It should be noted that the shunt isolation elements should be added at the symmetrical plane $A-A'$ so that they do not affect the even-mode responses. Meanwhile, in order to achieve a good impedance matching, multiple shunt isolation elements are adopted in this design. The shunt isolation elements can be resistors, capacitors, or inductors. As S_{22e} has been obtained from the even-mode analysis, it can be seen from (1c) and (1d) that the output port matching (S_{22} and S_{33}) and the isolation (S_{23}) will only depend on S_{22o} . From Fig. 6, since the feed lines, the resonators and the loaded capacitors have been determined from the even-mode circuit, S_{22o} has to be fulfilled by tuning the lumped elements R_1 , R_2 and L_i . Fig. 7 shows the optimized impedance matching at port 2 with different combinations of shunt elements ($R_1=200$ Ω , $R_2=100$ Ω and $L_i=100$ nH) under $C_1=1.2$ pF and $C_2=0.3$ pF. It can be seen that a good impedance matching can be easily achieved with multiple shunt elements. Fig. 8 shows the matching performance at port 2 with the optimized lumped elements when the loaded-capacitors vary. Good impedance matching has been maintained with different loaded capacitors C_1 and C_2 .

This article has been accepted for publication in a future issue of this journal, but has not been fully edited. Content may change prior to final publication in an issue of the journal. To cite the paper please use the doi provided on the Digital Library page.

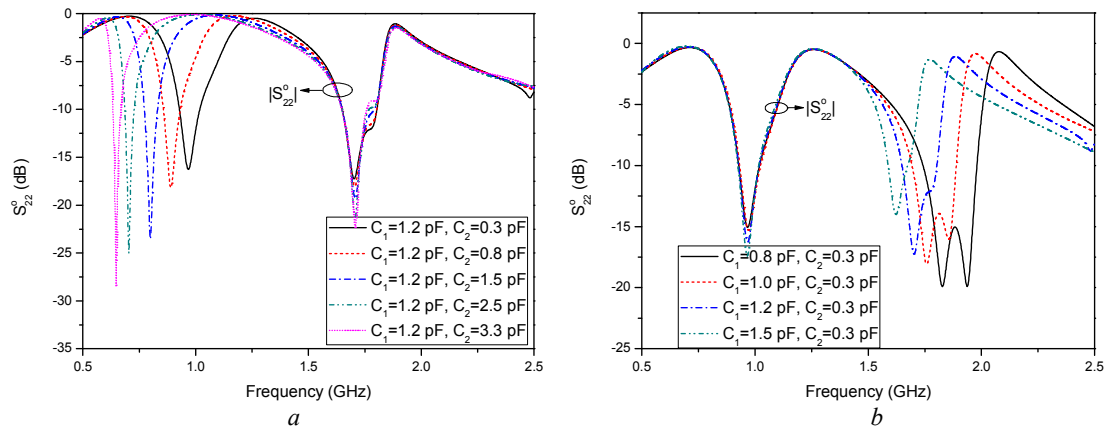


Fig. 8. Simulated S -parameters of the odd-mode circuit under different loaded-capacitors
a fixed C_1 and variable C_2 from 0.3 to 3.3 pF
b fixed C_2 and variable C_1 from 0.8 to 1.5 pF

3. Implementation and verification

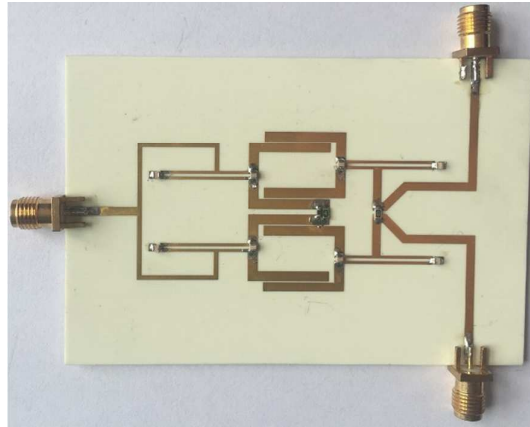


Fig. 9. Photograph of the fabricated circuit

After the even-and odd-mode circuits are analyzed, they can be combined to realize the dual-band filtering power divider shown in Fig. 1. For verification, a DB-FPD is fabricated on a Rogers 4350B substrate with a relative dielectric constant of 3.38, a thickness of 0.762 mm, and a dielectric loss tangent of 0.0027. The circuit dimensions are $L_1 = 13$ mm, $L_2 = 14$ mm, $L_3 = 5.7$ mm, $L_4 = 17.3$ mm, $L_5 = 6.15$ mm, $W_1 = 0.6$ mm, $W_2 = 2$ mm, $W_3 = 0.75$ mm, $W_4 = 1.7$ mm, $s_1 = 0.5$ mm, $s_2 = 0.2$ mm, and the lumped elements are $R_1 = 200 \Omega$, $R_2 = 100 \Omega$, and $L_i = 100$ nH. The overall size of the circuit is $0.41 \lambda_g \times 0.2 \lambda_g$, where λ_g is the guided wavelength at the center frequency of the lower passband with $C_2 = 0.3$ pF. The photograph of the fabricated device is shown in Fig. 9.

This article has been accepted for publication in a future issue of this journal, but has not been fully edited. Content may change prior to final publication in an issue of the journal. To cite the paper please use the doi provided on the Digital Library page.

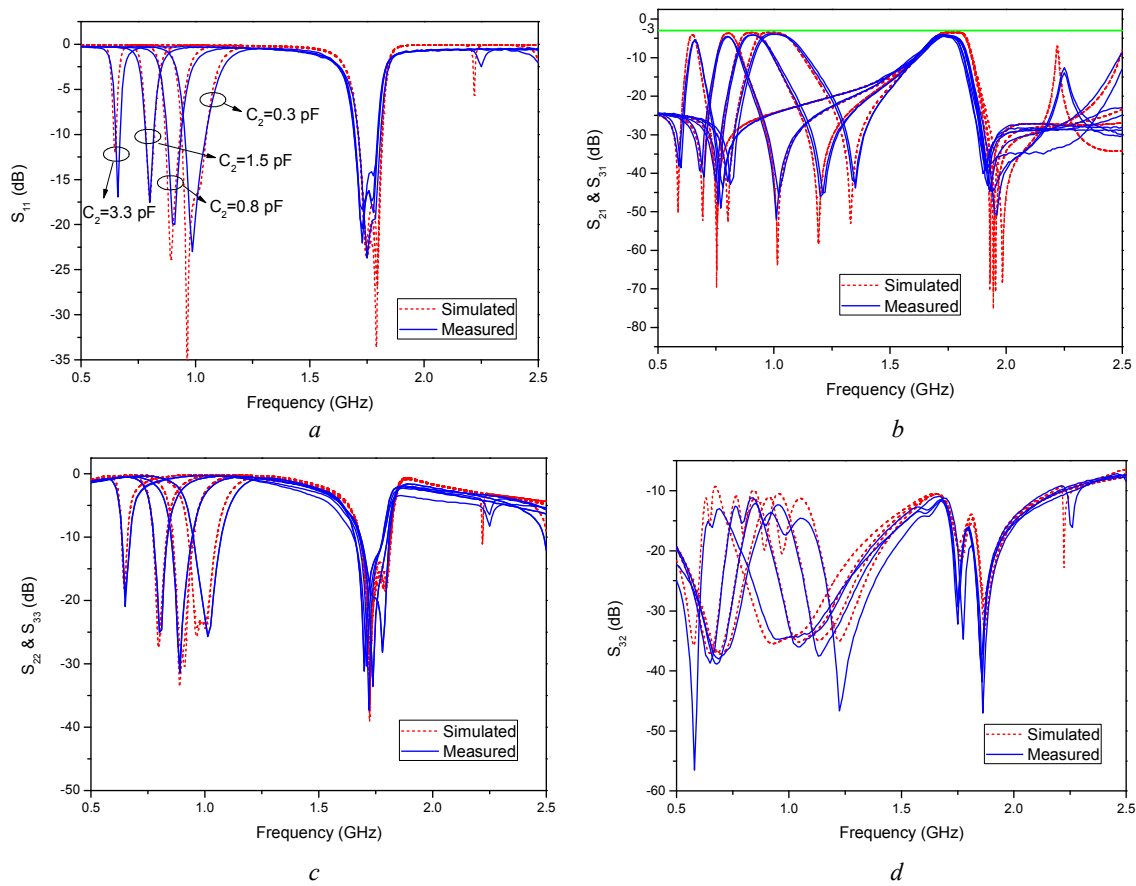


Fig. 10. Simulated and measured results when C_1 is fixed at 1.2 pF and C_2 varies

a S_{11}

b S_{21} & S_{31}

c S_{22} & S_{33}

d S_{32} .

The simulation is carried out using Ansoft HFSS, and the experimental results are measured using Agilent 8361C network analyzer. Four different values of C_1 (0.8 pF, 1.0 pF, 1.2 pF and 1.5 pF) and C_2 (0.3 pF, 0.8 pF, 1.5 pF and 3.3 pF) are used to test the performance and frequency controllability of the proposed DB-FPD. The measurement results agree well with the simulations. Fig. 10 shows the variation of the lower passband of the DB-FPD with C_2 . It is found that while the upper band is fixed at 1.74 GHz with $C_1=1.2$ pF and a 3-dB fractional bandwidth (FBW) of 9.2%, the lower band center frequency shows a tuning range of 40% from 0.99 GHz to 0.66 GHz when C_2 changes from 0.3 pF to 3.3 pF, The insertion loss varies from 3.81 dB to 5.32 dB (including the 3 dB power division loss).

This article has been accepted for publication in a future issue of this journal, but has not been fully edited. Content may change prior to final publication in an issue of the journal. To cite the paper please use the doi provided on the Digital Library page.

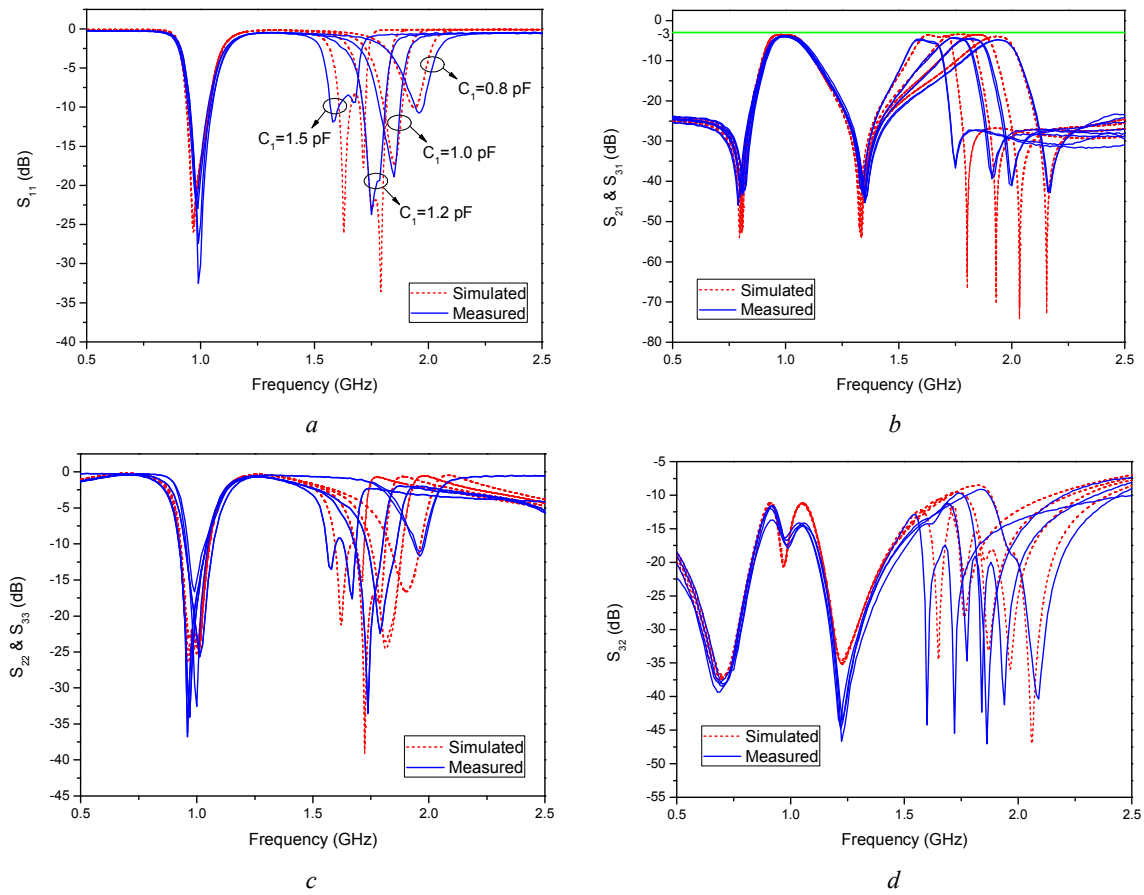


Fig. 11. Simulated and measured results when C_2 is fixed at 0.3 pF and C_1 varies

- a S_{11}
 b S_{21} & S_{31}
 c S_{22} & S_{33}
 d S_{32} .

Table 1. Comparison with some previously published works

References	Frequency (GHz)	FBW (%)	Insertion loss (dB)	In-band isolation (dB)	Adjustable frequencies	center	Tuning range (GHz)
[8] [#]	0.85	7.4	4.8	>17	Y		0.62-0.85
[16]	1.8/2.96	8.0/7.4	3.8/3.9	>8/10	N		-
[17] (Fig. 13)	0.276/0.483	22.1/8.9	3.97/4.65	>20/30	N		-
[18]	0.88/1.94	4.5/7.0	3.9/5.2	>10/10	N		-
[18]	3.5/5.0	7.4/4.2	3.9/4.9	>8/6	N		-
[19]	2.2/2.7	12.2/8.9	<3.5/3.5	>16/16	N		-
This work*	1.0/1.74	9.2/17.8	3.94/4.22	>12/12	Y		0.66-0.99 /1.6-1.94

[#] Reference [8] is a single-band tunable filtering power divider. The data in the table is obtained at $V_t = 5.2$ V.

*The data in the table correspond to $C_1 = 1.2$ pF and $C_2 = 0.3$ pF.

This article has been accepted for publication in a future issue of this journal, but has not been fully edited.

Content may change prior to final publication in an issue of the journal. To cite the paper please use the doi provided on the Digital Library page.

The measured performance variation of the upper passband is shown in Fig. 11. Similarly, while the lower band center frequency is fixed at 1.01 GHz with $C_2=0.3$ pF and a 3-dB FBW of 17.8%, the upper band center frequency can be tuned by 19.2% from 1.94 GHz to 1.60 GHz when C_1 changes from 0.8 pF to 1.5 pF. The insertion loss changes from 4.82 dB to 4.21 dB. Fig. 10 and Fig. 11 also show that the measured return loss at port 1, 2 and 3 are better than 10 dB in all states. The S_{23} is better than -12 dB for both the lower and upper passband in all cases, exhibiting good isolation between the output ports. Table 1 compares the proposed design with other published results in recent years. It can be seen that the proposed circuit demonstrates the ability of independently tuning the center frequencies of the dual bands, while maintaining comparable or improved electromagnetic performances.

4. Conclusion

In this paper, the CLCCLR based dual-band BPF is integrated with the PD to have achieved the dual functions of filtering and power division. By tuning the loaded-capacitors embedded in the resonators, the operating frequencies of the two passbands can be independently controlled. Two resistors and one inductor are added across the symmetrical plane to improve the isolation between the output ports. The even- and odd-mode method has been employed to analyze the performances of the dual-band filtering power divider. For verification, a prototype device is implemented. Simulated and measured results show good agreement. With the featured functions of dual-band filtering and power division, independently controllable center frequencies and compact size, the proposed circuit is attractive in applications in multiband wireless systems.

5. Acknowledgments

This work was supported in part by K.C. Wong Magna Fund in Ningbo University, and in part by Ningbo Natural Science Foundation (Grant no: 2016A610063) and National Natural Science Foundation of China (Grant no: 61571251).

6. References

- [1] Chappell, W. J., Naglich, E. J., Maxey, C., *et al.*: 'Putting the radio in Software-defined radio: Hardware developments for adaptable RF systems', *Proc. IEEE*, 2014, **102**, (3), pp. 307–320
- [2] Wong, S. W., Zhu, L.: 'Ultra-wideband power divider with good in-band splitting and isolation performances', *IEEE Microw. Wireless Compon. Lett.*, 2008, **18**, (8), pp. 518–520
- [3] Deng, P. H., Dai, L. C.: 'Unequal Wilkinson power dividers with favourable selectivity and high-isolation using coupled-line filter transformers', *IEEE Trans. Microw. Theory Tech.*, 2012, **60**, (6), pp. 1520-1529

This article has been accepted for publication in a future issue of this journal, but has not been fully edited.

Content may change prior to final publication in an issue of the journal. To cite the paper please use the doi provided on the Digital Library page.

- [4] Cheong, P., Lai, K., Tam, K.: 'Compact Wilkinson power divider with simultaneous bandpass response and harmonic suppression', *IEEE MTT-S Int. Microw. Symp. Dig.*, Anaheim, CA, USA, 23-28 May 2010, pp. 1588-1591
- [5] Song, K.: 'Compact filtering power divider with high frequency selectivity and wide stopband using embedded dual-mode resonator', *Electron. Lett.*, 2015, **51**, (23), pp. 1950–1952
- [6] Zhang, B., Liu, Y.: 'Wideband filtering power divider with high selectivity', *Electron. Lett.*, 2015, **51**, (6), pp. 495–497
- [7] Chen, C. F., Lin, C.-Y., Tseng, B.-H., *et al.*: 'Compact microstrip electronically tunable power divider with chebyshev bandpass response', in *Proc. Asia-Pacific Microw. Conf.*, Sendai, Japan, 4-7 Nov. 2014, pp. 1291–1293
- [8] Gao, L., Zhang, X. Y., Xue, Q.: 'Compact tunable filtering power divider with constant absolute bandwidth', *IEEE Trans. Microw. Theory Tech.*, 2015, **63**, (10), pp. 3505–3513
- [9] Zhang, X. Y., Wang, K.-X., Hu, B.-J.: 'Compact filtering power divider with enhanced second-harmonic suppression', *IEEE Microw. Wireless Compon. Lett.*, 2013, **23**, (9), pp. 483-485
- [10] Chen, C.-F., Huang, T.-Y., Shen, T.-M., *et al.*: 'Design of miniaturized filtering power dividers for system-in-a-package', *IEEE Trans. Comp., Packag., Manufact. Technol.*, 2013, **3**, (10), pp. 1663–1672
- [11] Lu, Y.-L., Wang, S., Dai, G.-L., *et al.*: 'Novel filtering power divider with external isolation resistors', *ETRI J.*, 2015, **37**, (1), pp. 61-65
- [12] Wang, K.-X., Zhang, X. Y., Hu, B.-J.: 'Gysel power divider with arbitrary power ratios and filtering responses using coupling structure', *IEEE Trans. Microw. Theory Techn.*, 2014, **62**, (3), pp. 431–440
- [13] Chen, F.-J., Wu, L.-S., Qiu, L.-F., *et al.*: 'A four-way microstrip filtering power divider with frequency-dependent couplings', *IEEE Trans. Microw. Theory Tech.*, 2015, **63**, (10), pp. 3494–3504
- [14] Rosenberg, U., Salehi, M., Amari, S., *et al.*: 'Compact multi-port power combination/distribution with inherent bandpass filter characteristics', *IEEE Trans. Microw. Theory Tech.*, 2014, **62**, (11), pp. 2659–2672
- [15] Li, Y. C., Xue, Q., Zhang, X. Y.: 'Single- and dual-band power divider integrated with bandpass filters', *IEEE Trans. Microw. Theory Tech.*, 2013, **61**, (1), pp. 69–76
- [16] García, R. G., Sánchez, R. L., Psychogiou, D., *et al.*: 'Single/multi-band Wilkinson-type power dividers with embedded transversal filtering sections and application to channelized filter', *IEEE Trans. Circuits Syst. I, Reg. Papers*, 2015, **62**, (6), pp. 1518–1527
- [17] Avrillon, S., Pele, I., Chousseaud, A., *et al.*: 'Dual-band power divider based on semi-loop stepped-impedance resonators', *IEEE Trans. Microw. Theory Tech.*, 2003, **51**, (4), pp. 1269–1273
- [18] Li, Q., Zhang, Y., Fan, Y.: 'Dual-band in-phase filtering power dividers integrated with stub-loaded resonators', *IET Microw. Antennas Propag.*, 2015, **9**, (7), pp. 695–699
- [19] Cai, C., Wang, J., Deng, Y., *et al.*: 'Design of compact dual-mode dual-band filtering power divider with high selectivity', *Electron. Lett.*, 2015, **51**, (22), pp. 1795–1796
- [20] Hong, J. S., Lancaster, M. J.: 'Microwave Filter for RF/Microwave Application' (Wiley, 2001)

This article has been accepted for publication in a future issue of this journal, but has not been fully edited.

Content may change prior to final publication in an issue of the journal. To cite the paper please use the doi provided on the Digital Library page.

- [21] Lu, Y.-L., Dai, G.-L., Li, E.-P., *et al.*: 'Dual-band bandpass filter using centrally coupled resonators (CCRs)', *J. Electromagnet. Waves Appl.*, 2013, **27**, (8), pp. 160–167
- [22] Zhang, X. Y., Xue, Q.: 'Novel centrally loaded resonators and their applications to bandpass filters', *IEEE Trans. Microw. Theory Tech.*, 2008, **56**, (4), pp. 913–921